

THE EFFECTS OF IRON CARBONYL-BASED CATALYST PRECURSORS ON THE REACTION OF 4-(NAPHTHYLMETHYL)BIBENZYL

Timothy D. Walter, Stephen M. Casey, Michael T. Klein, Henry C. Foley
Center for Catalytic Science and Technology
Department of Chemical Engineering
University of Delaware
Newark, DE 19716

ABSTRACT

The reaction pathways and kinetics of 4-(naphthylmethyl)bibenzyl (NBBM) were studied in an effort to resolve certain fundamentals underlying catalysis of coal liquefaction by Fe-based catalysts. Reaction of NBBM under a hydrogen atmosphere was performed for a series of iron carbonyl-based catalyst precursors: $\text{Fe}(\text{CO})_4\text{PPh}_3$, $\text{Fe}(\text{CO})_3(\text{PPh}_3)_2$, and $\text{Fe}(\text{CO})_2(\text{PPh}_3)_2\text{CS}_2$. The precursors' activities for the disappearance of NBBM were $\text{Fe}(\text{CO})_4\text{PPh}_3 > \text{Fe}(\text{CO})_2(\text{PPh}_3)_2\text{CS}_2 > \text{Fe}(\text{CO})_3(\text{PPh}_3)_2$. All precursors gave significantly higher rates than that for thermal reaction at 400°C. Thermolysis of NBBM was selective for cleavage at the bibenzyl bond, whereas the catalyst precursors were selective for cleavage at the naphthyl moiety. Hydrogenation activity was also observed for each of the three catalyst precursors. Possible catalytic reaction mechanisms are considered.

INTRODUCTION

Direct coal liquefaction is the process of fragmenting the coal structure into lower molecular weight materials. Thermal liquefaction is accompanied by bond-making retrograde reactions, which can result in a more refractory solid than the original coal. This poor thermal selectivity to desirable products motivates the use of a catalyst to increase the rate and selectivity of liquefaction.

Much of the microporous coal structure¹ is not accessible to classical solid catalyst particles. This suggests that the use of homogeneous or fine particle catalysts, which would better access the pore structure and, in turn, the surface area of coal, could be promising for catalysis of coal reactions. The two key coal liquefaction reaction families of bond scission and hydrogenation could thus occur for coal, and not only coal-derived liquids.

Our continuing work has focused on iron-based materials. In particular, catalyst precursors that are able to form fine particle iron and iron sulfides at coal liquefaction conditions have been sought. To consider the effect of the precursor's ligands on the activity of the catalyst, the series $\text{Fe}(\text{CO})_4\text{PPh}_3$, $\text{Fe}(\text{CO})_3(\text{PPh}_3)_2$, and $\text{Fe}(\text{CO})_2(\text{PPh}_3)_2\text{CS}_2$ of triphenylphosphine (PPh₃)-substituted iron carbonyls has been examined.

The evaluation of these catalysts involved extensive model compound reaction chemistry. This is because simple model systems, individually, mimic some of the important structural features in coal, which enables the examination of specific bond reactivities in coal. The use of well-defined hydrocarbon systems also allows focus to be placed on the catalyst and its role. The model compound 4-(naphthylmethyl)bibenzyl (NBBM) mimics some of the important attributes of coal, e.g., a fused two-ring aromatic connected to other aromatics by short alkyl chains. However, its structure, illustrated in Figure 1, is simple enough to allow for quantitative analysis.

Two studies of the reaction of NBBM have been published. Farcasiu, et al.² reacted NBBM with the hydrogen donor 9,10-dihydrophenanthrene (DHP) thermally and in the presence of a catalytic carbon material. They observed products from thermal fission of each of the bonds labeled in Figure 1, followed by radical capping with DHP derived hydrogen. Reaction with the carbon catalyst increased NBBM conversion and showed, upon subtraction of the thermal background, nearly 100% selectivity to bond A scission. The thermal and catalytic (catalyst precursor $\text{Fe}(\text{CO})_3(\text{PPh}_3)_2$) reactions of NBBM under both hydrogen and nitrogen atmospheres at 420 °C have been examined by Walter et al.³ They classified the main products from reaction of NBBM into three major classes: bond A scission products, bond D scission products, and

hydrogenation products. Walter et al.³ proposed a reaction scheme that consists of the rupture of the thermally weak bond D, followed by bond A cleavage through ipso-substitution of a benzyl radical and subsequent liberation of a methylbenzyl radical. Bond A scission products are naphthyl phenyl methane (from benzyl ipso-substitution), naphthalene, tetralin, methyl bibenzyl and p-xylene (secondary product from methylbibenzyl). Bond D scission products are 4-(naphthylmethyl)toluene and toluene, and hydrogenation products are hydrogenated NBBM species (e.g., 1,2,3,4-tetrahydro NBBM). The stoichiometry for bond A scission was consistent with ipso-substitution by benzyl and H[•] radicals, since the sum of the molar yields of naphthyl phenyl methane, naphthalene and tetralin is equal to the sum of the molar yields of methylbibenzyl and p-xylene.

The objective of the present paper is to report on the reaction of NBBM in the presence of a series of substituted iron-carbonyl catalyst precursors at 400°C under a hydrogen atmosphere. We first describe the preparation of the catalytic materials, followed by a description of the reaction system and procedures. Quantitative kinetics are examined through a lumped reaction network. A consistent catalytic reaction mechanism, consisting of the insertion of catalytically bound hydrogen into the naphthalene ring leading to bond A scission and/or hydrogenation, is discussed.

EXPERIMENTAL

Preparation of Catalytic Materials: The reagents for the synthesis of the catalysts, triphenylphosphine (99%, Aldrich), Fe(CO)₅ (99.5%, Alfa Research Chemicals) and Fe₂(CO)₉ (99.7%, Alfa Research Chemicals), were used as received. All solvents were distilled under N₂ over 4 Å molecular sieve to remove oxygen and water, and reactions were performed under an atmosphere of purified nitrogen in Schlenk-type glassware to exclude air and water.

Fe(CO)₄PPh₃ Synthesis: Fe(CO)₄PPh₃ was prepared by a combined photochemical and thermal route from triphenylphosphine (PPh₃) in iron pentacarbonyl (Fe(CO)₅), following the synthesis procedure of Conder and Darensbourg⁴. This preparation procedure, which is selective to the monosubstituted product, is outlined in Figure 2a. Thus, 3 g of PPh₃ (0.011 mole) was added to 28 ml of Fe(CO)₅ (0.208 mole) under a dry N₂ atmosphere. The stirred solution was irradiated with a 100-Watt long-wave UV lamp for 2 hours. The lamp was then turned off and the solution was held at reflux conditions (100°C) for one hour, followed by an additional hour of reflux with the UV lamp turned on. At the end of the reaction sequence, excess Fe(CO)₅ was removed in vacuo. The residue was extracted with 50 ml THF and separated on a neutral alumina chromatography column in air, eluting with 75 ml THF. 50 ml of distilled water was then added and the solution volume reduced under vacuum to precipitate pale yellow crystals that were collected by filtration and purified by recrystallization from heptane. The above procedure gave a 50% yield of Fe(CO)₄PPh₃ (based on PPh₃). The product was identified through melting point comparison, 198-200°C (lit.⁵: 201-203°C) and spectroscopy, IR: ν(CO) (CH₂Cl₂): 2051, 1974, 1939 cm⁻¹ (lit.⁸ ν(CO) (CHCl₃): 2059, 1978, 1938 cm⁻¹).

Fe(CO)₃(PPh₃)₂ Synthesis: Fe(CO)₃(PPh₃)₂ was prepared from Fe(CO)₅ and PPh₃ in refluxing cyclohexanol, following the procedure of Clifford and Mukherjee⁶ outlined in Figure 2b. In this synthesis, 2 ml of Fe(CO)₅ (0.015 mole) and 5 g of PPh₃ (0.018 mole) were added to 100 ml of cyclohexanol. The solution was then refluxed (161°C) for 1 hour under N₂. 100 ml of hexane was added to the reaction solution which was then cooled, giving a yellow precipitate. This relatively straightforward procedure gave a 39% yield (based on Fe(CO)₅) of the disubstituted product, Fe(CO)₃(PPh₃)₂, with a small amount of the monosubstituted derivative, Fe(CO)₄PPh₃, present, which was removed by silica gel chromatography. The product was identified through melting point comparison, 265-285°C (lit.⁸: 272°C) and spectroscopy, IR: ν(CO) (CH₂Cl₂): 1882 cm⁻¹ (lit.⁸: ν(CO) (CHCl₃): 1887 cm⁻¹).

Fe(CO)₂(PPh₃)₂CS₂ Synthesis: Fe(CO)₂(PPh₃)₂CS₂ was prepared from diiron nonacarbonyl (Fe₂(CO)₉) and PPh₃ in refluxing (46°C) carbon disulfide (CS₂), as outlined by

Baird et al.⁷ The route is outlined in Figure 2c. A mixture of 1.5 g of $\text{Fe}_2(\text{CO})_9$ (0.004 mole) and 3 g of PPh_3 (0.011 mole) in 25 ml of CS_2 was refluxed under N_2 for 40 minutes. The solution was cooled, and the rust-red solid, $\text{Fe}(\text{CO})_2(\text{PPh}_3)_2\text{CS}_2$, was precipitated by addition of diethylether (~5-10% yield based on $\text{Fe}_2(\text{CO})_9$). The product was identified through melting point comparison, 133°C (lit.¹⁰: 130-134°C) and spectroscopy, IR: $\nu(\text{CO})$ (CH_2Cl_2): 1990, 1929 cm^{-1} (lit.¹⁰: $\nu(\text{CO})$ (CHCl_3): 1989, 1929 cm^{-1}).

NBBM Reactions: NBBM (TCI Americas), dichloromethane (Fisher Scientific) and all other chemicals (Aldrich Chemical Company) were used as received. The reactions were carried out in 7 cm^3 stainless steel microbatch reactors. The reactant and catalyst precursor were placed in an open 10 x 75 mm glass tube within the reactor to prevent wall interactions. The loadings of NBBM and catalyst precursor were 50 mg and 1.4 wt% by iron, respectively (5 mg for $\text{Fe}(\text{CO})_4\text{PPh}_3$, 8 mg for $\text{Fe}(\text{CO})_3(\text{PPh}_3)_2$, 8.3 mg for $\text{Fe}(\text{CO})_2(\text{PPh}_3)_2\text{CS}_2$), and all reactions took place under 1000 psig (cold) hydrogen pressure. The reactor was pressurized to 1000 psig with hydrogen and then discharged three times prior to heat up. This ensured reaction in the absence of air. The reactor was then plunged into a fluidized sand bath at 400°C and, after the passage of the reaction time, removed from the sandbath for cooling in an ice bath for at least 30 minutes. A known amount of biphenyl was then added to the contents of the glass tube, which was subsequently diluted with dichloromethane. The mixture was then separated in a Hewlett-Packard 5890 Gas Chromatograph with Flame Ionization Detector and a Hewlett-Packard 5890 Gas Chromatograph with a Hewlett-Packard 5970 Mass Selective Detector. Both Gas Chromatographs used Hewlett-Packard Ultra 2 columns (crosslinked 5% Ph Me Silicone) with dimensions 50 m x 0.2 mm and 0.33 mm film thickness.

RESULTS AND DISCUSSION

The reactions of NBBM were studied at 400 °C under 1000 psig (cold) hydrogen pressure in the presence of each of the catalyst precursors ($\text{Fe}(\text{CO})_4\text{PPh}_3$, $\text{Fe}(\text{CO})_3(\text{PPh}_3)_2$, $\text{Fe}(\text{CO})_2(\text{PPh}_3)_2\text{CS}_2$) and in the absence of a catalytic precursor.

The disappearance kinetics shown in Figure 3 reveal that the three catalyst precursors had significant activity above the thermal baseline for the disappearance of NBBM. $\text{Fe}(\text{CO})_4\text{PPh}_3$ led to the highest conversion over most of the reaction times. Conversion in the presence of $\text{Fe}(\text{CO})_2(\text{PPh}_3)_2\text{CS}_2$ was initially lower than in the presence of $\text{Fe}(\text{CO})_3(\text{PPh}_3)_2$, but by 60 minutes the trend had reversed.

Figure 4 is a plot of the yields of the three product classes, i.e., bond A scission, bond D scission and hydrogenation products, versus NBBM conversion for reaction at 400°C in the presence of the three catalyst precursors. The predominate activity for bond A scission and NBBM hydrogenation is clear. Figure 4 shows that, for the catalyst precursor $\text{Fe}(\text{CO})_4\text{PPh}_3$, the rate of appearance of bond A scission products decreases markedly between 120 and 150 minutes. There was very little NBBM left in the reaction mixture at this point (Figure 3); however, there was a significant amount of hydrogenated NBBM (Figure 4). The stoichiometry for bond A scission during reaction with each of the three catalyst precursors at 400 °C was consistent with the results observed by Walter et al.³ and discussed earlier. Ipso-substitution by either benzyl or H^\cdot radicals can account for the observed product distributions.

Figure 5 is a simple reaction network that describes NBBM reaction in terms of the three product lumps: bond A scission products, bond D scission products and NBBM hydrogenation products. The network also includes an "other products" lump, which accounts for products not identified through gas chromatography, e.g., gases and high molecular weight products. Two additional product classes account for secondary reactions to hydrogenated versions of products attributed to bond A and bond D scission.

Quantitative kinetics analysis was accomplished by optimizing network predictions against the experimental data. Table 1 contains the best-fit values of first-order rate constants obtained by parameter estimation using a simplex optimization routine. Model predictions, with the experi-

mental data, for NBBM consumption are shown in Figure 6. The fits are good for reaction thermally and in the presence of $\text{Fe}(\text{CO})_3(\text{PPh}_3)_2$. However, for reaction in the presence of $\text{Fe}(\text{CO})_4\text{PPh}_3$ and $\text{Fe}(\text{CO})_2(\text{PPh}_3)_2\text{CS}_2$ the fits are poor, due to highly non-first order behavior.

The rate constants do provide insight into the reaction mechanisms. The values for the bond D scission constants, k_D , are independent of the presence of the three catalysts. That is, k_D for reaction with any of the catalysts is not significantly different than that during thermal reaction. This suggests that bond D scission is purely thermal and is unaffected by the presence of a catalyst. Similarly, the values for the bond A scission constants, k_A , are similar for reaction with each of the three catalysts and quite different than that for thermal reaction. This suggests that a single mechanism is responsible for the bond A scission in the presence of the three catalyst precursors. In addition, the values of the hydrogenation constants, k_H , are consistent with the higher hydrogenation activity observed for $\text{Fe}(\text{CO})_4\text{PPh}_3$ catalyst than for the other two shown in Figure 4. Also, the slower scission of bond A in hydrogenated NBBM relative to that for bond A scission of NBBM is reflected in the relationship $k_{\text{HA}} < k_A$ for all three catalyst precursors. Finally, all three catalyst precursors showed higher activity for hydrogenation of naphthalene (k_{AH}) than for hydrogenation of the substituted naphthalene (k_{H}).

Mechanistic insights derive from the known activity of reduced iron as an effective hydrogenation catalyst. The iron likely dissociates hydrogen into atoms that can, in turn, add to the naphthyl ring. When a hydrogen inserts at the ipso position, a thermochemically favorable β -scission pathway affords naphthalene and a methylbenzyl radical. This proposed mechanism is also consistent with the lack of bond A scission of hydrogenated NBBM. The destruction of the electron rich naphthalene system both decreases the molecule's ability to interact with the catalyst and removes the electronic topology required for ipso-substitution.

CONCLUSIONS

The catalytic chemistry of NBBM at 400°C under a hydrogen atmosphere in the presence of the series of iron-carbonyl based catalyst precursors $\text{Fe}(\text{CO})_4\text{PPh}_3$, $\text{Fe}(\text{CO})_3(\text{PPh}_3)_2$ and $\text{Fe}(\text{CO})_2(\text{PPh}_3)_2\text{CS}_2$ was examined. The three catalyst precursors showed significant activity for the disappearance of NBBM above the thermal baseline. Two of the main product classes were "bond A scission" and "NBBM hydrogenation". Quantitative network analysis examined the kinetics for each reaction family among the catalyst precursors. This analysis indicated that: bond D scission was purely thermal and unaffected by the presence of the catalyst precursors; bond A rate constants were similar for reaction in the presence of all three catalyst precursors and different from that for thermal reaction; and the hydrogenation rate constant was higher for $\text{Fe}(\text{CO})_4\text{PPh}_3$ than for the other two catalyst precursors. A consistent reaction mechanism involves catalytic dissociation of H_2 into hydrogen atoms, which are, in turn, inserted into the naphthalene system of NBBM; the naphthalene site at which the hydrogen atom is inserted determines the outcome of bond A scission or hydrogenation. The slower rate of bond A scission observed by the hydrogenated NBBM species can be qualitatively explained with decreased catalyst interaction and removal of ipso-substitution electronic topology.

ACKNOWLEDGMENT

We would like to thank Dr. William H. Calkins, Dr. G. Alex Mills and Dr. Malvina Farcasiu for discussions in the area of coal chemistry and coal catalysis, and Dennis Kalaygian for his help in performing some of the NBBM reaction experiments. This work was supported by the United States Department of Energy Grant DE-AC22-90PC90050.

¹ Larsen, John W., Wernett, Patrick, "Pore Structure of Illinois No. 6 Coal", *Energy & Fuels*, **2** (5), 719-720, 1988

² Farcasiu, Malvina, Smith, Charlene, "Modeling Coal Liquefaction, 1. Decomposition of 4-(1-Naphthylmethyl)benzyl Catalyzed by Carbon Black", *Energy & Fuels*, **5**(1), 83-87, 1991

³ Walter, Timothy D., Casey, Stephen M., Klein, Michael T., Foley, Henry C., "Reaction of 4-(naphthylmethyl)biphenyl Thermally and in the Presence of $\text{Fe}(\text{CO})_2(\text{PPh}_3)_2$ ", submitted for publication, Presented at DOE Liquefaction Contractors' Meeting, Pittsburgh, PA Sept. 22-24, 1992

⁴ Conder, H.L., and Darensbourg, M. York, "The Synthesis of Group V Substituted Derivatives of Iron Pentacarbonyl in High Yield", *J. Organomet. Chem.*, 1974, **67**, 93-97.

⁵ Cotton, F.A. and Parish, R.V., "The Stereochemistry of Five-coordinate Compounds. Part I. Infrared Spectra of Some Iron(0) Compounds", *J. Chem. Soc.*, 1960, 1440-1446.

⁶ Clifford, A.F., and Mukherjee, A.K., "Iron Carbonyl Complexes of Triphenylphosphine, Triphenylarsine, and Triphenylstibine", *Inorg. Chem.*, 1963, **2**, No. 1, 151-153.

⁷ Baird, M.C., Hartwell, jun., G., and Wilkinson, G., "Carbon Disulphide Complexes of Vanadium, Iron, Cobalt, Ruthenium, and Iridium; the Preparation of trans-Bis(triphenylphosphine)thiocarbonylhalogeno-rhodium(I) and -rhodium(III) Complexes", *J. Chem. Soc. (A)*, 1967, 2037-2040.

	$(\text{k}_1 / \text{s}^{-1}) \times 10^5$			
	Thermal	$\text{Fe}(\text{CO})_4\text{PPh}_3$	$\text{Fe}(\text{CO})_3(\text{PPh}_3)_2$	$\text{Fe}(\text{CO})_2(\text{PPh}_3)_2\text{CS}_2$
k_A	0.455	4.32	3.00	4.19
k_H	0.035	15.8	5.59	6.59
k_D	0.457	0.366	0.454	0.363
k_{AH}	4.92	42.4	18.2	17.8
k_{DH}	1.83	4.44	6.36	8.87
k_{HA}	0.112	1.72	1.33	0.549
k_{HD}	0.031	0.505	0	0
k_O	1.11	5.91	2.78	2.99

Table1: Regressed values for the first-order rate constants for the reaction network of Figure 5.

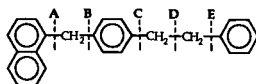
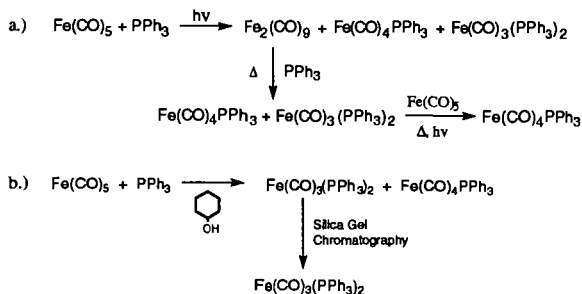


Figure 1: Model compound, 4-(naphthylmethyl)biphenyl.



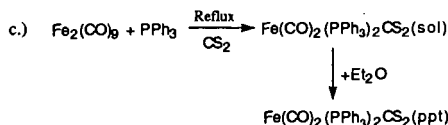


Figure 2: Synthesis routes for: a) $\text{Fe}(\text{CO})_4\text{PPh}_3$; b) $\text{Fe}(\text{CO})_3(\text{PPh}_3)_2$; $\text{Fe}(\text{CO})_2(\text{PPh}_3)_2\text{CS}_2$.

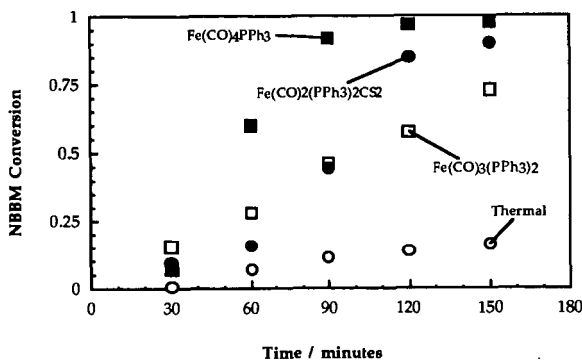


Figure 3: Kinetics of NBBM disappearance at 400°C under 1000 psig H_2 (cold) in the presence of iron carbonyl based catalyst precursors.

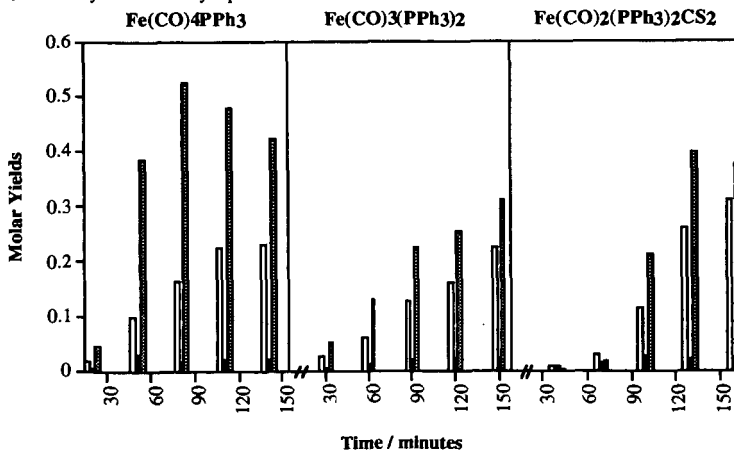


Figure 4: Molar yields of bond A scission, bond D scission and NBBM hydrogenation products classes upon reaction of NBBM at 400°C under 1000 psig H_2 (cold) in the presence of iron carbonyl based catalyst precursors. □ Bond A Scission Products; ■ Bond D Scission Products; ▨ Hydrogenation Products.

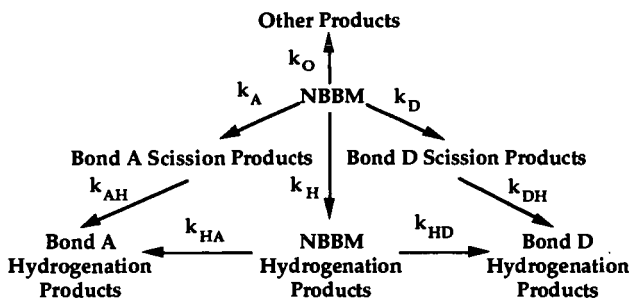


Figure 5: Lumped network for the reaction of NBBM at 400°C under 1000 psig H₂ (cold) in the presence of iron carbonyl based catalyst precursors.

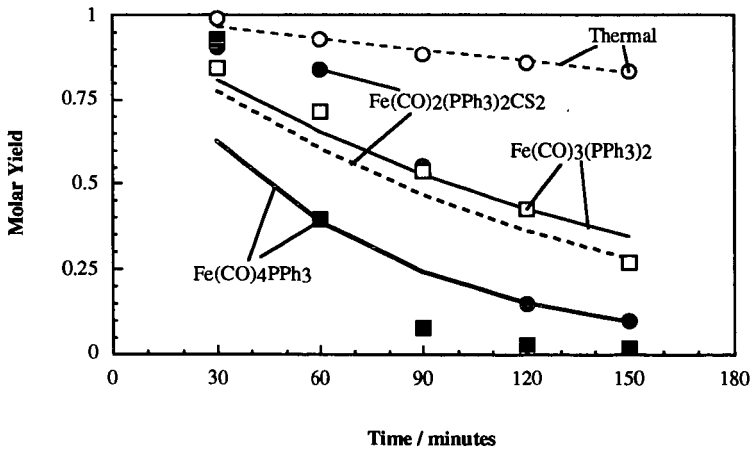


Figure 6: Model fits for the lumped network describing the reaction of NBBM at 400°C under 1000 psig H₂ (cold) in the presence of iron carbonyl based catalyst precursors. The lines are the predicted curves and the points are the experimentally measured values.